Controlling morphology, mesoporosity, crystallinity, and photocatalytic activity of ordered mesoporous TiO_2 films prepared at low temperature

Björn Elgh,[1] Ning Yuan,[1] Hae Sung Cho,[2] David Magerl,[3] Martine Philipp,[3] Stephan V. Roth,[4] Kyung Byung Yoon,[5] Peter Müller-Buschbaum,[3] Osamu Terasaki,[2] and Anders E. C. Palmqvist[1]

[1]*Applied Surface Chemistry, Department of Chemical and Biological Engineering, Chalmers University of Technology, SE 412 96 Göteborg, Sweden*
[2]*Graduate School of EEWS (WCU), KAIST, Daejeon 305-701, South Korea*
[3]*Lehrstuhl für Funktionelle Materialien, Physik-Department, Technische Universität München, 85748 Garching, Germany*
[4]*DESY, Notkestrasse 85, 22603 Hamburg, Germany*
[5]*Department of Chemistry, Sogang University, Seoul 121-742, South Korea*

(Received 1 August 2014; accepted 12 October 2014; published online 27 October 2014)

Partly ordered mesoporous titania films with anatase crystallites incorporated into the pore walls were prepared at low temperature by spin-coating a microemulsion-based reaction solution. The effect of relative humidity employed during aging of the prepared films was studied using SEM, TEM, and grazing incidence small angle X-ray scattering to evaluate the mesoscopic order, porosity, and crystallinity of the films. The study shows unambiguously that crystal growth occurs mainly during storage of the films and proceeds at room temperature largely depending on relative humidity. Porosity, pore size, mesoscopic order, crystallinity, and photocatalytic activity of the films increased with relative humidity up to an optimum around 75%. [http://dx.doi.org/10.1063/1.4899117]

The last decades have seen photocatalysis emerge as an appealing alternative for solar energy harvesting,[1] carbon dioxide reduction,[2] removal of organic pollutants,[3] and self-cleaning surfaces. The ability to completely degrade organic pollutants into carbon dioxide and water makes photocatalysis an attractive alternative for purification of contaminated waters and air. Solar energy is abundant on the surface of the Earth, and the prospect of using photocatalysis for conversion of solar energy into energy carriers such as hydrogen or methanol is appealing in a world faced with an increasing demand for sustainable energy systems. Since the first discovery by Fujishima and Honda,[1] titania is the most extensively investigated of all photocatalysts. Titania exists mainly in the three polymorphs anatase, rutile, and brookite. Of these, anatase is generally considered to be the most photocatalytically active[3] although rutile has been found to exhibit significant activity,[4] while amorphous titania shows low or no activity.[5] The photocatalytic activity of brookite is less investigated due to difficulties in synthesizing phase-pure brookite. However, some reports show that brookite displays high photocatalytic activity.[6,7]

In the early nineties, researchers at Mobil oil reported a new concept for preparing ordered mesoporous materials. Using supramolecular surfactant assemblies as templates, hexagonal (MCM-41), cubic (MCM-48), and lamellar (MCM-50), mesoporous silicas were synthesized.[8,9] Further development of these systems made tuning of pore size possible by using large amphiphilic block copolymers.[10–14] These types of materials have received much interest from the research community due to the numerous potential applications in, e.g., separation technology, drug release, and heterogeneous catalysis. Nowadays, a plethora of ordered mesoporous materials with different elemental compositions and structural properties have been reported. Transition metal oxide-based materials constitute one of the most interesting families of ordered mesoporous materials and it has attracted much

attention due to the possibly unique properties of these materials. Mesoporous titania has received special attention for photovoltaic and photocatalytic applications where large specific surface area, controllable pore size and morphology, and high interparticle connectivity are desired properties.

Antonelli *et al.* were the first to synthesize mesoporous titania using a surfactant-templated process.[15] Typically, such prepared mesoporous titania exhibits amorphous pore walls due to the low temperature nature of templated syntheses since temperatures in excess of 350 °C are usually needed to achieve crystallization of the pore walls.[16,17] For photocatalytic applications, crystalline titania is much preferred. However, the stability of ordered mesoporous titania at such high temperatures is often too low, which results in loss of the meso-ordered structure and even collapse of the pore structure.[16] Low temperature synthesis routes are rare and typically require specially tailored titania precursors.[18–20] In an effort to bypass the crystal growth-induced collapse of the mesoporous structure, mesoporous and ordered mesoporous materials have been prepared by surfactant-assisted co-assembly of nanoparticles.[21,22] However, this method results in low interparticle connectivity, which reduces the photovoltaic and photocatalytic efficiency of these materials.[21]

Recently, Nilsson *et al.* reported a direct low temperature synthesis route for hexagonally ordered mesoporous titania films with anatase crystallites incorporated in the pore walls based on commercial titania precursors.[23] Crystallites were formed and grown in a reverse micellar solution containing a triblock copolymer, which was later spin-coated onto a glass substrate utilizing the evaporation induced self-assembly (EISA) process[24] to form a liquid crystalline phase. The fundamentals of titania crystallization and its impact on the formation of mesophases in this new and unique system have been outlined in two recent studies.[25,26] These studies suggest that crystal growth not only occurs in the formed reversed micellar solution but also continues within the hydrophilic domains of the liquid crystal template formed in the film preparation process. They also show that crystallinity and type of crystal polymorph formed are highly sensitive to common synthesis parameters such as reaction time and pH. This crystal formation and growth process, at or near room temperature, clearly distinguishes this synthesis approach from previously employed synthesis routes since it allows for tailoring titania properties by tuning synthesis variables not otherwise available. The prospects of such a synthesis are interesting as it offers the possibility to be tuned to different crystal polymorphs, crystallite sizes, crystallinities, and mesostructures.

It has been shown that a mixture of anatase and rutile is most beneficial for photocatalytic activity.[27] However, the difficulties in preparing pure ordered mesoporous titania with pore walls fully or partly consisting of rutile via high-temperature routes have so far not been surmountable. Low-temperature crystallization routes to ordered mesoporous titania may offer means to pore walls consisting of the high-temperature polymorph rutile, while still retaining the integrity of the ordered pore structure. Therefore, it is vital to understand the details of the formation mechanism and the parameters affecting this synthesis for further development of tailored materials.

The photocatalytic activity of ordered mesoporous titania films has been studied earlier.[28–32] However, these studies have this far mainly been restricted to materials in which crystallization of the pore walls was achieved by high-temperature treatment. Recently, we studied the photocatalytic properties of ordered mesoporous films with anatase crystallites in their pore walls prepared at low temperature and investigated the impact of storage time of the reaction solution prior to film formation.[25] The films showed an increased photocatalytic activity with an increased storage time, ascribed to a larger degree of crystallinity and crystallite size. Although the degree of mesoporosity is important in providing access to high specific surface area and facile transport of reactants and products to and from the catalyst surface, the degree of order of the mesopores appeared less important than crystallinity for the photocatalytic performance of the films.

Studies of other types of surfactant-templated titania films have revealed the importance of water present both in the synthesis mixture and in the surrounding environment. Thus, the relative humidity (RH) has been found an important parameter during formation and subsequent storage of those materials.[17,33] To date, the effect of RH during aging of ordered mesoporous titania films prepared as reported by Nilsson *et al.*, has not yet been investigated. In the present work, we show that the relative humidity applied during aging of mesoporous TiO_2 films prepared using this method has strong effects on crystallinity, mesoscopic order, and morphology of the films. We also relate the variations in these properties to differences in their photocatalytic activity.

Nonionic ethylene oxide (EO) propylene oxide (PO) ethylene oxide (EO) triblock copolymer Pluronic™ F-127 ($EO_{100}PO_{70}EO_{100}$, M_w = 12700 g/mol), hydrochloric acid (37%), titanium n-butoxide (97%) were all purchased from Sigma Aldrich, and ethanol (99.5%) was purchased from Solveco and used in the synthesis of titania films as previously reported by Nilsson *et al.* but under different conditions of relative humidity.[23] In a typical synthesis, a reverse micellar phase was formed containing 3 g of ethanol, 2.25 g of Pluronic™ F-127, and 1.5 g of 5 M hydrochloric acid. To this mixture, 1.5 g of titanium n-butoxide was added dropwise. The mixture was stirred with a magnetic stirrer for 15 min, during which a clear reverse micellar phase was obtained. The closed reaction container was stored at 313 K for 6 h. After storage, 400 ml of the reaction solution was spin-coated onto microscope glass slides at 300 rpm for 5 s followed by 1000 rpm for 10 s. The spin-coated films were aged in a controlled humidity box for at least 3 days. Trays with moisturized salts present in the humidity box were used to control the relative humidity. The humidity inside the box was monitored for the duration of the aging process using a hygrometer from Testo. The time between spin-coating and introduction into the controlled environment never exceeded 15 min. After aging, the organic template and residues of solvent and organic reaction products were removed by treating the films in a UV/ozone oven for 24 h.

Transmission electron microscope (TEM) images were taken with a JEOL JEM-4010 operated at 400 kV. TEM specimens were prepared by scraping material off of the prepared films and dispersing the material in ethanol. The sample/ethanol dispersion was dropped onto a microgrid and dried. Scanning electron microscope (SEM) images were taken with a JSM-7600F operated at 1 kV (accelerating voltage: 3 kV, specimen bias: 2 kV) and 2.7 mm working distance. SEM specimens were prepared by fixating powder scraped off of the film to the SEM sample holder using carbon paste. The mesoscopic structure and the density of the porous titania films were investigated by grazing incidence small angle X-ray scattering (GISAXS).[34] The GISAXS measurements were performed at the MiNaXS beamline P03 at HASYLAB at DESY, Hamburg, Germany.[35] The sample-to-detector distance was chosen to be 2.61 m, and the wavelength of the X-ray beam was 0.095 nm. The samples were each illuminated for 150 s, and the 2D scattering data were recorded with a Pilatus 300k detector. The 2D scattering data were evaluated by performing two types of cuts. The vertical cut, along the q_z-axis at $q_y = 0$, comprises amongst others the so-called Yoneda-peak,[36] which is positioned at the critical angle of the investigated material. As the critical angle of a given material is directly related to its electron density, the detector cut allows estimating the mass density of the porous titania films. Moreover, the horizontal cut, performed at the critical angle for the porous titania along the q_y-axis, gives information about lateral structures inside the films.[37]

Photocatalytic activity measurements of the as-prepared titania films were performed in a homemade flow-through microreactor made from Teflon™ with an online UV/Vis spectrometer (GBC Cintra-30). The reactor is fitted with an optical window coated with F-doped SnO_2 (FTO) with a cut-off wavelength of approximately 300 nm. The total volume of the reactor setup was 4 ml, and the irradiated sample area was 2 cm^2. A 100 W high-pressure Hg-lamp was used as irradiation source, and light was focused onto the sample area with a set of lenses and apertures. An USB2000 Ocean optics® spectrometer fitted with an optical fiber was used to measure the photon power at the sample position. The photon power was measured between the wavelengths 300 and 400 nm and was 4.3 mW/cm^2 with a variation between runs smaller than 1.5%. The temperature of the reaction solution was monitored over the initial 2 h with a Eurotherm thermocouple and found to be stable at 296 K. The photocatalytic activity of the films was evaluated for phenol degradation. A water solution containing 0.1 mM phenol was exposed to the irradiated films for 5 h, during which the phenol concentration was monitored with UV/Vis spectroscopy following the 270 nm absorption peak of phenol.

In this work, we have investigated the effects of the relative humidity during aging of mesoordered titania films prepared by spin-coating reverse micellar solutions in which titania nanocrystals are formed. A reverse micellar phase was prepared based on the ternary phase diagram of the triblock copolymer Pluronic™ F127/butanol/water system, shown in Figure 1, and redrawn from Holmqvist *et al.*[38] This phase diagram does not completely represent the synthesis mixture used, but is currently the best available. Hence, a mixture was prepared with the composition 3:2.25:1.5:1.5 weight ratio of ethanol:F127:5 M HCl:titanium n-butoxide.

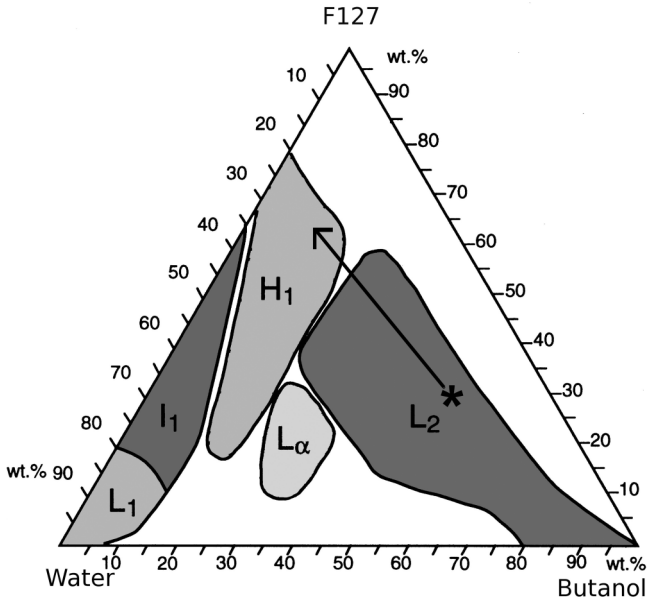

FIG. 1. Ternary phase diagram redrawn from Holmqvist *et al.*[38] Based on the assumption that ethanol acts as part of the oil phase together with the butanol released upon hydrolysis of titanium n-butoxide, the reaction mixture is initially in the reverse micellar phase with a composition represented by a star in the phase diagram. Rapid evaporation of solvent during the spin-coating of the sample films moves the system into the hexagonal H_1 phase of the phase diagram indicated by the arrow.

Assuming that ethanol acts as oil together with the butanol released upon hydrolysis of the titanium alkoxide, the mixture will have a composition that is represented by the star in the phase diagram shown in Figure 1. The reason for using ethanol instead of butanol is its easier evaporation exploited in the subsequent step of the synthesis. After mixing the ethanol, polymer, and acid, the resulting solution was a transparent single phase supporting that a reverse micellar L_2 phase was formed as suggested from the phase diagram. Upon addition of the titania precursor, a sudden white precipitate formed but quickly disappeared again giving a clear and transparent solution. This observation can be explained by the formation of titanium-hydroxo-aquo species upon addition and hydrolysis of the titanium n-butoxide and the subsequent rapid peptization of these species. The formulated reaction mixture was, thereafter, stored at 313 K for 6 h in a 50 ml capped polypropylene flask. During this storage the titania hydrolysis products undergo condensation reactions by which titania nanoparticles form and grow successively larger over time.[23] After storage, the reaction mixture was spin-coated onto glass substrates during which the rapid evaporation of the solvent shifts the system into the hexagonal H1 phase of the ternary phase diagram illustrated in Figure 1, forming an organic/inorganic composite according to the EISA concept.[23] Clearly, the system is still highly dynamic during the spin-coating process since the phase transition from a reverse micellar phase to normal hexagonal phase necessitates a shift from a hydrophobic to a hydrophilic continuous phase. Such a shift is associated with large conformational changes and would be severely hampered if the titania had undergone extensive condensation or aggregation prior to the spin-coating. A series of spin-coated films were prepared as summarized in Table I. The films were then stored for 3 days at ambient temperature in a controlled environment but at different relative humidities of 3.8%, 12%, 45%, 75%, and >95%, respectively.

Following removal of the organic template, SEM images were collected on mesoporous TiO_2 films A-D described in Table I. Representative images are shown in Figures 2(a)–2(d). Film D clearly exhibits pores within the mesorange arranged in an ordered fashion consistent with a hexagonal mesostructure cleaved along, as well as perpendicular to, the pore channels. The diameter of the pores as well as the thickness of the pore walls are both estimated to be 5 nm based on the SEM micrographs, in good agreement with earlier observations.[23] A micrograph of film C is displayed in Figure 2(c). At the surface of the material, mesopores are clearly visible. However, the alignment

TABLE I. Conditions used to prepare mesoporous TiO_2 films. Storage time refers to time after spin-coating, and relative humidity refers to the value in the surrounding environment during storage of the films.

Film	Storage time (days)	Relative humidity (%)
A	3	3.8
B	3	12
C	3	45
D	3	75
E	3	>95

of the pores is poor and no ordered arrangement of the pore openings could be discerned. In film B, pores with a diameter around 5 nm were regularly found, whereas no pores were found in film A, as shown in Figures 2(a) and 2(b). Thus, neither of these two latter samples shows mesoscopic order. The SEM analysis shows that the relative humidity employed during aging of the sample films has a strong influence on their final morphology and mesoscopic order and that a high relative humidity is essential for the development of the templated inorganic mesostructure. We find that a relative humidity around 75% is beneficial for the mesoscopic order. Crepaldi *et al.* showed that the relative humidity plays multiple roles during and closely after film formation for another EISA-type templated synthesis of mesostructured TiO_2 films.[33] They suggested that a suitable relative humidity sustains a high fluidity of the film and, thus, allows for the formation of a liquid crystalline phase also affecting the curvature of the micelles by incorporation or elimination of water.[33] In addition,

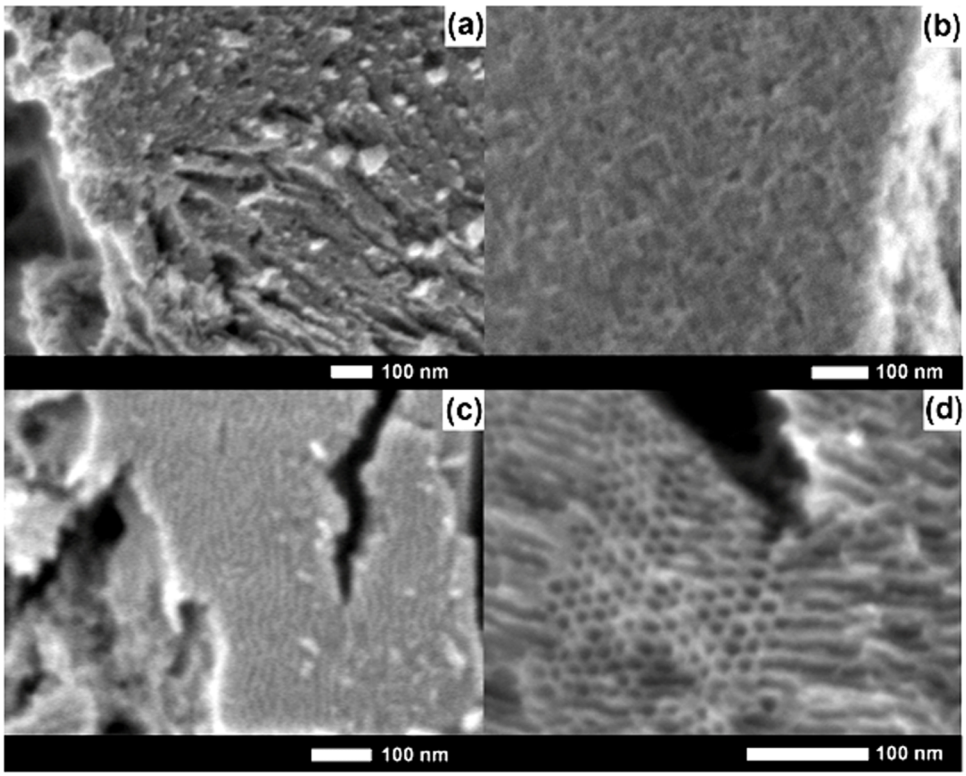

FIG. 2. SEM micrographs of films A-D prepared as described in Table I. (a) Film A aged at a RH of 3.8% shows no mesoscopic order. (b) Film B aged at a RH of 12% shows no mesoscopic order but mesopores are clearly visible. (c) Film C aged at RH of 45% shows worm-like channels oriented along the surface of the particle but no clear pore openings. (d) Film D aged at a RH of 75% shows a clear mesoscopic order with pore openings arranged in a hexagonal pattern as well as straight pore channels.

it promotes the exchange between water and hydrochloric acid increasing the condensation rate necessary for the formation of a stable inorganic framework. It is important to realize the influence of the acid concentration on the condensation/polymerization reactions forming the templated inorganic film. Inorganic titania species in water establish an equilibrium between Ti-aquo, -hydroxo, and -oxo complexes. The dominating complex is set mainly by pH, where the equilibria are shifted from oxo complexes at high pH to hydroxo complexes at intermediate pH and aquo complexes at low pH.[39] Condensation of titania complexes at an intermediate pH favouring aquohydroxo-ligands will preferentially occur by olation as shown in Eq. (1).[39]

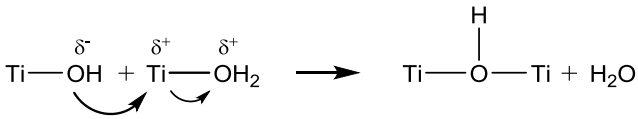

(1)

Olation occurs by nucleophilic substitution where the hydroxy group is the nucleophile and the aquo-ligand is the leaving group. In highly acidic media, the equilibrium is strongly shifted towards aquo-ligands. Aquo-ligands are excellent leaving groups but poor nucleophiles. Thus, the condensation of titania will be severely hampered due to the lack of good nucleophiles, allowing the system longer time to self-assemble into an ordered mesophase.[39] Interestingly, film E was not amenable for characterization and evaluation because the high relative humidity of >95% used, did not allow for a proper film to form. Instead, the highly humid environment rendered the film liquid-like with most of the solid material of the film aggregated at the edges of the substrate creating a highly uneven film. This observation illustrates the strong influence of the equilibrium between water in the prepared films and the surrounding air.

To gain more detailed structural information of the films, they were probed with GISAXS. The horizontal cuts through the 2D GISAXS data, shown in Figure 3(a), give access to the lateral structures present on a mesoscopic length scale within the porous titania films. These cuts were fitted using a model of two types of cylinders having a radial distribution, each type of cylinder being distributed as a 1D-paracrystal in the film.[40] The local monodisperse approximation was taken into account.[41] The modelled cylinder diameters of the small cylinders are attributed to the diameters of the pores, whereas the distance related to the 1D-paracrystal is ascribed to the center-to-center distance between the pores of the titania films. A second larger type of cylinders is only present with a very low probability and a broad size distribution. We attribute this second cylinder type to clusters of different sizes within the film. As shown in Figure 3(b), the pore size as well as the pore distance increases with an increasing relative humidity. The radii indeed vary from 2.5 nm for film A to 4.0 nm for film D aged at 75% relative humidity. For films B, C, and D, the pore dimensions deduced from GISAXS and SEM agree well within the error bars. That this is not the case for

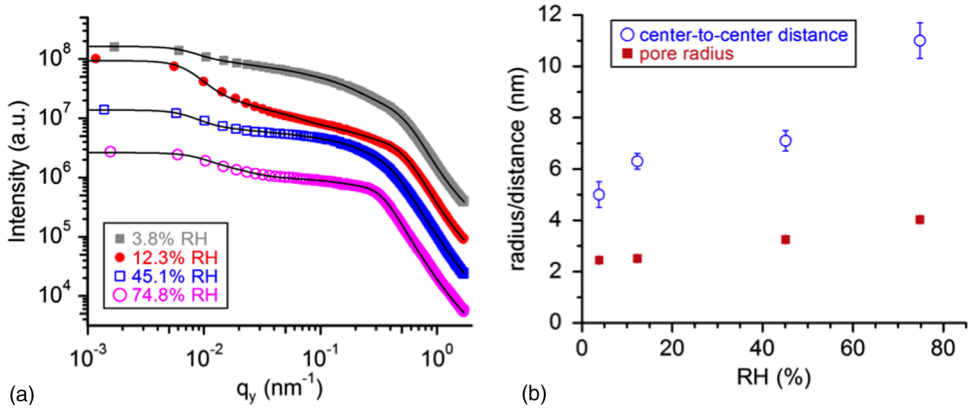

FIG. 3. (a) Horizontal cuts through the 2D GISAXS data performed at the critical angle of four porous titania films. The solid lines are fits to the data as described in the text. The data are shifted along the intensity axis for clarity. (b) Pore radius and center-to-center distances obtained from the fits.

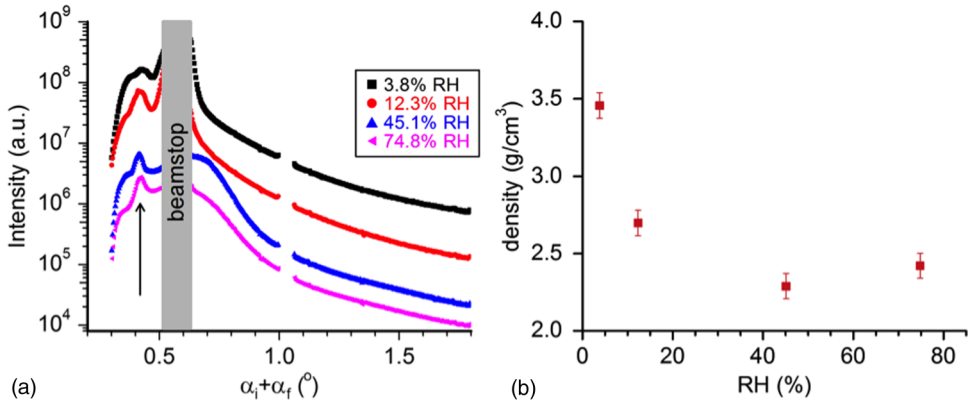

FIG. 4. (a) Vertical cuts through the 2D GISAXS data of the four porous titania films. The data are shifted along the intensity axis for clarity. The specular reflection is shielded by a beamstop. (b) Mass density versus relative humidity for four porous titania films, as deduced from the position of the Yoneda peak in (a) (shown by the arrow).

film A, may be related to the fact that the X-ray beam is able to penetrate into the bulk of the film and, hence, GISAXS averages over different and much larger sample volumes than SEM.

The vertical cuts of the 2D GISAXS data are depicted in Figure 4(a). As described in the above section, the position of the Yoneda peak (marked by an arrow) may be used to determine the mass density of the porous titania films. Figure 4(b) reveals that aging under higher relative humidity increases the porosity of the films and, hence, reduces the density of the films. Apparently, film A prepared under very low relative humidity conditions possesses a much higher density than the films prepared with increased relative humidity. This again confirms the strong influence of the relative humidity during aging of the mesoporous TiO_2. Further increasing the relative humidity does not have much effect on the overall mass density of the film but changes the surface of the film, as witnessed by the SEM images in Figure 2. Unfortunately, the type of ordered mesoscopic phase present in film D was not possible to determine with GISAXS. Most likely, the ordered domains of the prepared films are too small and mixed with areas of disordered pores.

It is known that the growth of nanoparticles in the formulated micellar solution is a slow process that proceeds over several days. However, the exact size of the nanoparticles formed in the reaction mixture during the storage process was not possible to determine while in solution. An analysis of the degree of crystallisation and the TiO_2 nanoparticle growth rate was done by recovery of the formed nanoparticles by centrifugation at 60 000 rpm for 3 h followed by repeated washing with ethanol. The amount of organic matter in the recovered sample was determined by thermogravimetric analysis and the total yield of TiO_2 nanoparticles formed could, thus, be calculated. At 20 h of reaction, the total yield was found to be as low as 2% of the total amount of titanium added. Hence, it is clear that at the point of spin-coating, which was at 6 h of reaction in the microemulsion, the TiO_2 crystallite growth process is still at an early stage, and the solution then consists of very small TiO_2 particles and with the major fraction of the titania precursor still solubilized in the solution.

High resolution transmission electron microscopy (HR-TEM) micrographs of films A and D were collected and analysed to assess the effect of the relative humidity under aging of the prepared films on their crystallinity. Films A and D represent the extreme points of the studied series of samples with a relative humidity of 3.8% and 75%, respectively. The TEM micrographs of film A shown in Figures 5(a) and 5(b) display only very few TiO_2 crystallites and film A can, thus, be regarded largely amorphous. In agreement with the SEM analysis, no mesoscopic order was observed in the TEM micrographs of film A. In contrast, Figures 5(c) and 5(d) show TEM images of film D, which display large areas of ordered mesopores consistent with hexagonal ordering and pore diameters around 5 nm and visible lattice fringes of crystallites between 2 and 5 nm present in the pore walls. Figure 5(e) shows a magnification of one crystallite, clearly exposing crystal lattice fringes. Figures 5(f) and 5(g) show FFT images of Figures 5(d) and 5(e), respectively. These are in

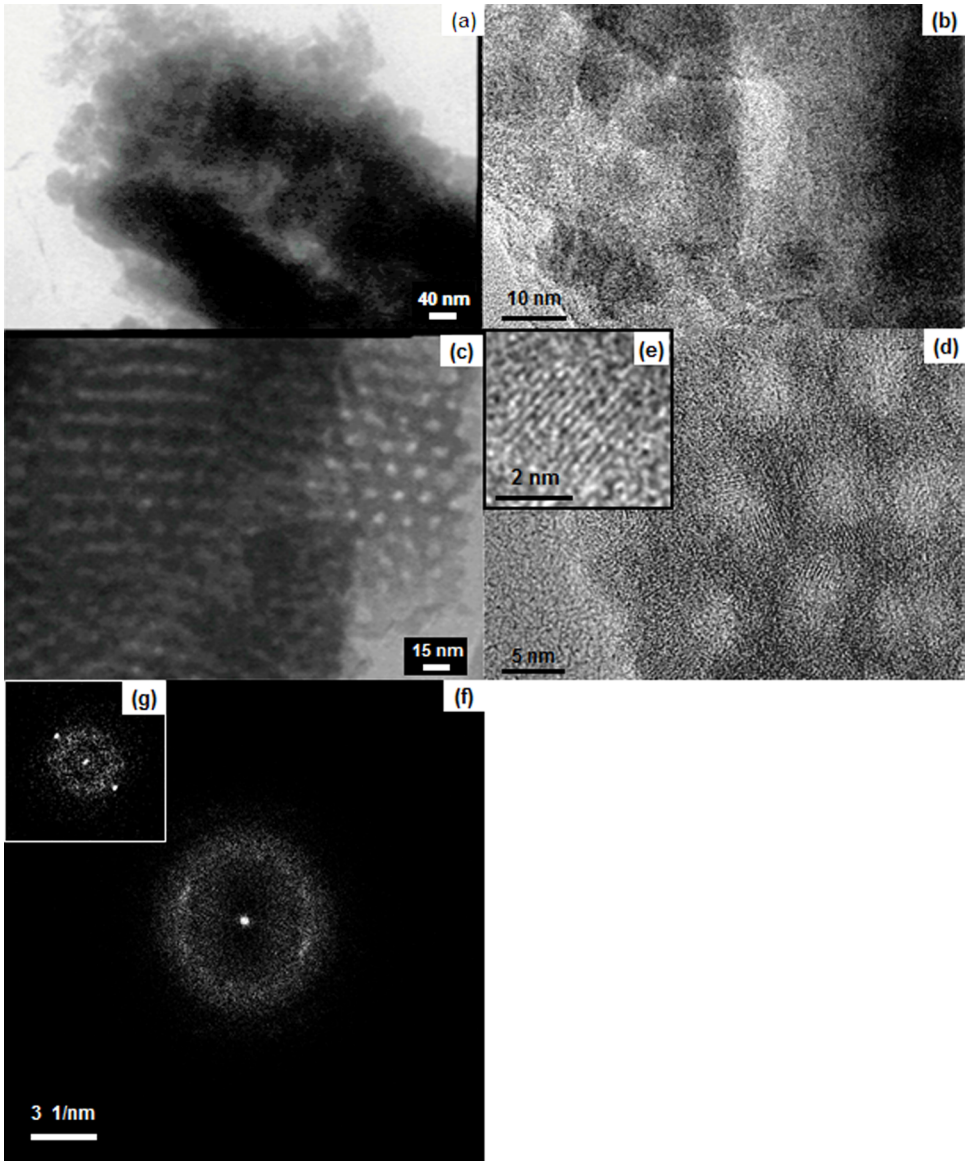

FIG. 5. TEM micrographs of mesoporous TiO_2 films A and D, aged at 3.8% and 75% relative humidity, respectively. (a) TEM image of film A, (b) HR-TEM image of film A showing very few crystallites, (c) TEM image of film D, (d) HR-TEM image of sample D showing lattice fringes of anatase crystallites with a diameter of 2–5 nm and pores with a diameter of approximately 5 nm arranged in a hexagonal pattern. (e) Magnification of one crystallite from (d) showing lattice fringes with 3 Å separation. (f) and (g) are FFT images of (d) and (e), respectively. Due to the small number of coherent crystallite regions, (f) shows spotty Debye ring. The radius of the first Debye ring corresponds to the d-spacing of 0.313 nm for the (101) plane of TiO_2 anatase phase.

agreement with previous electron diffraction studies of a mesoporous TiO_2 film prepared according to an identical procedure, which revealed that the TiO_2 crystallites are of the anatase polymorph.[23] It has been explained with a mechanism in which crystallites, preformed during treatment of the reaction mixture at slightly elevated temperature, are incorporated into the hydrophilic pore walls of the liquid crystalline inorganic/organic composite prepared.[23] Furthermore, our recently published study of a similar but disordered model system suggests that besides the crystallites preformed in the reaction mixture, crystallization and growth of nanoparticles can also occur within the hydrophilic domains of the liquid crystal template.[26] The fact that the two films studied here contain so strikingly different degrees of crystallinity provides new and important insight into the formation mechanism of the anatase crystallites of this system. If the crystallites present in the pore walls of

film D were formed solely prior to the EISA step, we would expect to observe them also in film A since the synthesis procedure and storage time prior to spin-coating are identical for the two films. However, the results presented here show, instead, conclusively that the growth of the anatase crystallites occurs mainly within the hydrophilic domains of the liquid crystalline inorganic/organic composite during the storage of the spin-coated films as suggested in our previous study.[26] Also, if extensive crystal growth would occur in the reaction solution prior to the formation of the hexagonal liquid crystal template, the formed particles would hamper the large conformational changes necessary for the phase transition from a reverse micellar phase to a hexagonal phase. Furthermore, the results establish that this growth of the anatase crystallites is highly dependent on the relative humidity of the environment where the films are stored. Considering the large difference in crystallinity between films A and D, the possibility that the anatase crystallites present within the pore walls of film D are caused by the UV/ozone treatment used to remove the surfactant, can be ruled out, since similar amounts of crystallites then would have been expected to be present also in film A. Apparently this crystallite growth depends strongly on the balance between the water content in the film and the surrounding environment in a parallel way to the dependence discussed for the organization of the mesostructure.

Upon spin-coating, the concentration of the soluble titania precursors will increase due to the removal of the solvent. This will increase the supersaturation of the soluble species and promote their condensation to solid films. The exchange between water from the surrounding atmosphere and hydrochloric acid present in the film will be greatly affected by the relative humidity. If the acidity decreases, as is expected by a higher relative humidity, a more rapid condensation of titania intermediates occurs. However, the formation and growth of crystallites during aging of the films is not independent of the preceding step of storing the reaction mixture before spin-coating. Previous studies of crystal growth in similar systems and under similar conditions show that the formation and growth of crystallites do, in fact, occur in the reverse micellar solution and that the duration of the microemulsion storage affects the final crystallite size in the films.[23,25,42] The results obtained here, thus, prove a mechanism in which the crystallite nucleation initiates and is followed by some particle growth during the storage stage of the micellar reaction mixture at 313 K,where most of the crystallite growth takes place inside the subsequently prepared spin-coated liquid crystal template at 293 K via a process that is highly dependent on the relative humidity of the environment in which the film is stored.

The photocatalytic performance of the mesoporous TiO_2 films was evaluated by measurements of phenol degradation rates in a microreactor upon illumination of the films with UV light. The general mechanism for the photocatalytic degradation of phenol over anatase has been reported elsewhere and is not discussed here.[43,44] However, it is of interest to note the general appearance of the UV/Vis spectra of the solution during the degradation of phenol shown in Figure 6. As the degradation of phenol proceeds, there is a decrease in the phenol absorption band at 270 nm and a build-up in absorption around 240 nm for all films. Similar observations have previously been reported by Andersson *et al.*[4] They reported a new absorption band at 245 nm under photocatalytic degradation of phenol, which was observed using anatase phase titania but not using the rutile polymorph.[4] This absorption band has been ascribed to the intermediate formation of benzoquinone.[44]

Figure 7 shows the fraction of phenol degraded ($1 - C/C_0$) versus time of UV illumination for films A-D as well as the fraction of phenol degraded for all samples after 5 h of UV exposure. The photocatalytic activity for phenol degradation is clearly higher for films stored at a high relative humidity after spin-coating. In this work, a relative humidity of 75% during aging was found to be the optimum for achieving films with high photocatalytic activity for degradation of phenol. The small peculiar initial decrease in $1 - C/C_0$ for film A in Figure 7 is likely an effect of phenol polymerization known to be caused by photolysis reactions of phenol.[45] The relative humidity was also found to greatly affect the crystallinity, porosity, mesoscopic order, and pore size of the prepared films, all of which may influence the photocatalytic activity of the films. The film with the highest photocatalytic activity showed the highest degree of crystallinity, the widest pore diameter, the highest degree of meso-order, and among the two highest porosities of the films studied. The film with the lowest photocatalytic activity was prepared with the lowest relative humidity. This film showed the lowest degree of crystallinity and meso-order, the smallest pore diameter, and the lowest

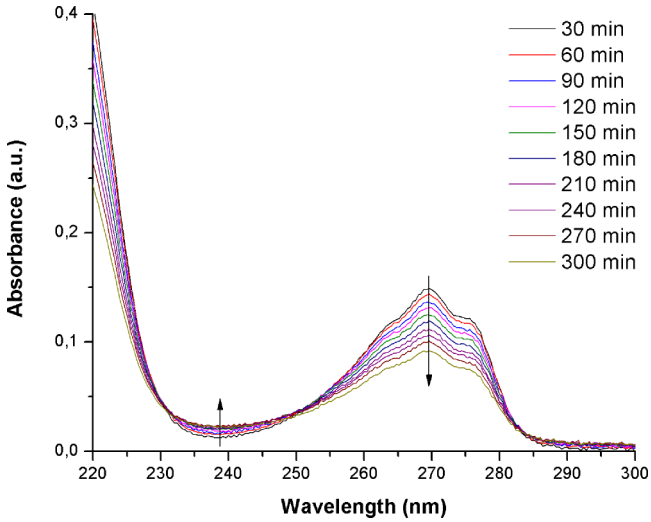

FIG. 6. UV/Vis spectra of the phenol/water reaction solution during the course of the photocatalytic activity measurement of film D aged at a RH of 75%. The phenol degradation is monitored by the decrease in the 270 nm absorption band of phenol. The absorption band at 210 nm is also ascribed to phenol but is not used to follow the degradation of phenol due to the risk of interference of particle scattering and degradation product. Seen at 245 nm is the buildup of a new absorption band ascribed to intermediate phenol degradation products.

porosity. It is, hence, not possible to unambiguously determine which of these materials properties are the most important for the photocatalytic activity of the films based only on the data available here. However, a large specific surface area is generally beneficial for a photocatalyst as the surface represents the interface of charge transfer reactions. The surface of the photocatalyst has also been suggested to serve as the locus for trapped electrons and holes, thus providing sites for prolonging the lifetime of the separated electron-hole pairs by hampering their recombination.[46] Even though it has been impossible to measure the specific surface area directly for any of the films investigated in this work, it is reasonable to assume that the films with the highest porosity will also have the highest specific surface areas. The increase in porosity follows the same trend as the photocatalytic activity; as the porosity increases so does the photocatalytic activity. The possible effect of pore size on the photocatalytic activity for the evaluated sample series may be due to differences in diffusion rate of phenol in pores with diameters ranging from 2 to 4 nm. Whether diffusion of phenol is the rate-limiting step of the photocatalytic degradation of phenol in mesoporous materials is unknown.

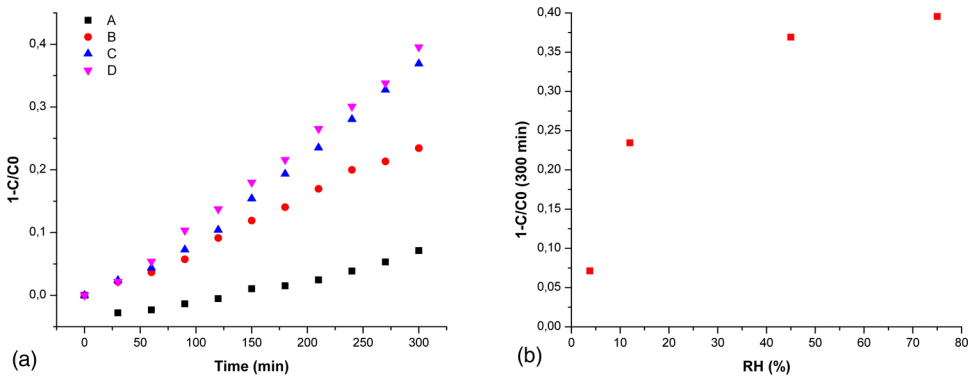

FIG. 7. (a) The photocatalytic activity of mesoporous TiO_2 films A-D aged at different relative humidities illustrated as fraction of phenol degraded versus time of UV illumination. The initial decrease of $1 - C/C_0$ for film A aged at 3.8% relative humidity is likely an effect of phenol photolysis. In (b) the fraction of phenol degraded at 300 min of reaction is shown for films A-D as a function of the relative humidity during storage of the spin-coated films.

However, several authors have observed an increase in photocatalytic activity with an increased light intensity for titania photocatalysts, suggesting that the generation and diffusion of electrons and holes to the surface of the photocatalyst is the reaction rate limiting process.[47,48] As is evident from HR-TEM micrographs, the amount of crystallites increases with an increased relative humidity used during aging. It is known that amorphous titania shows little or no catalytic activity,[5] this is why the increase in crystallinity is expected to have a profound effect on the activity of the evaluated sample films. This is also evident from the activity measurements of the investigated sample films for which an increase in crystallinity results in an expected increase in activity as is illustrated in Figures 7(a) and 7(b). Increasing the relative humidity up to 75% during aging of the prepared films, thus, has a positive influence on several properties beneficial for the photocatalytic activity.

The synthesis of mesoporous titania films prepared at low temperature from a micellar reaction mixture via EISA methodology has been studied and the photocatalytic activity of the prepared films evaluated. The relative humidity employed during aging of the prepared films showed profound effects on mesoscopic order, porosity, pore size, crystallinity, and photocatalytic activity of the films. An increased porosity, as well as an increase in the pore diameter from 2 to 4 nm was observed as the relative humidity was increased from 3.8% to 75%. Ordered mesopores were only observed in SEM and TEM for the film aged at 75% relative humidity. Even though the ordered domains of mesopores were too small to give rise to Bragg diffraction peaks in GISAXS measurements, the horizontal cuts of the 2D GISAXS data showed an increased ordering for films prepared at high relative humidity. HR-TEM micrographs revealed the critical impact of relative humidity for the formation of anatase crystals incorporated into the pore walls of the prepared films. For films aged at a relative humidity of 75%, anatase crystallites were readily found incorporated into the pore walls, whereas for films aged at 3.8% few or no crystallites could be found. This shows the critical importance of relative humidity of the environment around the EISA films for the formation of crystalline pore walls at room temperature. It also elucidates important details of the formation mechanism of this new type of materials synthesis, where it is now unambiguously concluded that the major part of the crystallization occurs in the films after the EISA step. Photocatalytic activity towards phenol degradation was observed to progressively increase for films aged at higher relative humidity up to 75%. We suggest that this increase is caused by an increase in the crystallinity of the films aged at higher relative humidity and possibly by a more easily accessible catalyst surface. Furthermore, the growth of crystallites within the hydrophilic domains of the liquid crystal template may offer the means to develop synthesis routes to ordered mesoporous titania films with rutile crystallites incorporated into the porewalls.

This work has been carried out with support from the Danish Centre for Energy Materials funded by the Danish Council for Strategic Research. A.E.C.P. thanks the Swedish Research Council (VR) for financial support of a Senior Researcher position. O.T. thanks VR, the Knut and Alice Wallenberg Foundation and World Class University Program (R-31-2008-000-10055-0) of the Ministry of Education, Science, and Technology in Korea for support. P.M.-B. thanks the Bavarian State Ministry of Sciences, Research and Arts for funding this research work via TUM.solar in the frame of the Bavarian Collaborative Research Project "Solar technologies go Hybrid" (SolTec). M.P. thanks the Fonds national de la Recherche (Luxembourg) for receipt of an AFR Postdoc grant cofunded under the Marie Curie Actions of the European Union. K.B.Y. thanks National Research Foundation of Korea, Project No. 2012M1A2A2671784.

[1] A. Fujishima and K. Honda, "Electrochemical photolysis of water at a semiconductor electrode," Nature **238**, 37–38 (1972).
[2] K. Kočí, L. Obalová, L. Matějová, D. Plachá, Z. Lacný, J. Jirkovský, and O. Šolcová, "Effect of TiO_2 particle size on the photocatalytic reduction of CO_2," Appl. Catal., B **89**, 494–502 (2009).
[3] M. R. Hoffmann, S. M. Martin, W. Choi, and D. W. Bahneman, "Environmental applications of semiconductor photocatalysis," Chem. Rev. **95**, 69–96 (1995).
[4] M. Andersson, L. Österlund, S. Ljungström, and A. Palmqvist, "Preparation of nanosize anatase and rutile TiO_2 by hydrothermal treatment of microemulsions and their activity for photocatalytic wet oxidation of phenol," J. Phys. Chem. B **106**, 10674–10679 (2002).
[5] B. Ohtani, Y. Ogawa, and S.-I. Nishimoto, "Photocatalytic activity of amorphous–anatase mixture of titanium(IV) oxide particles suspended in aqueous solutions," J. Phys. Chem. B **101**, 3746–3752 (1997).
[6] A. D. Paola, G. Cufalo, M. Addamo, M. Bellardita, R. Campostrini, M. Ischia, R. Ceccato, and L. Palmisano, "Photocatalytic activity of nanocrystalline TiO_2 (brookite, rutile and brookite-based) powders prepared by thermohydrolysis of $TiCl_4$ in aqueous chloride solutions," Colloids Surf., A **317**, 366–376 (2008).

[7] B. Ohtani, J.-I. Handa, S.-I. Nishimoto, and T. Kagiya, "Highly active semiconductor photocatalyst: Extra-fine crystallite of brookite TiO_2 for redox reaction in aqueous propan-2-ol and/or silver sulfate solution," Chem. Phys. Lett. **120**, 292–294 (1985).
[8] C. T. Kresge, M. E. Leonowicz, W. J. Roth, J. C. Vartuli, and J. S. Beck, "Ordered mesoporous molecular sieves synthesized by a liquid-crystal template mechanism," Nature **359**, 710–712 (1992).
[9] J. S. Beck, J. C. Vartuli, W. J. Roth, M. E. Leonowicz, C. T. Kresge, K. D. Schmitt, C. T.-W. Chu, D. H. Olson, E. W. Sheppard, S. B. McCullen, J. B. Higgins, and J. L. Schlenkert, "A new family of mesoporous molecular sieves prepared with liquid crystal templates," J. Am. Chem. Soc. **114**, 10834–10843 (1992).
[10] D. Zhao, J. Feng, Q. Huo, N. Melosh, G. H. Fredrickson, B. F. Chmelka, and G. D. Stucky, "Triblock copolymer syntheses of mesoporous silica with periodic 50 to 300 angstrom pores," Science **279**, 548–552 (1998).
[11] M. Rawolle, M. A. Ruderer, S. M. Prams, Q. Zhong, D. Magerl, J. Perlich, S. V. Roth, P. Lellig, J. S. Gutmann, and P. Müller-Buschbaum, "Nanostructuring of titania thin films by a combination of microfluidics and block-copolymer-based sol–gel templating," Small **7**, 884–891 (2011).
[12] M. Rawolle, M. A. Niedermeier, G. Kaune, J. Perlich, P. Lellig, M. Memesa, Y.-J. Cheng, J. S. Gutmann, and P. Müller-Buschbaum, "Fabrication and characterization of nanostructured titania films with integrated function from inorganic–organic hybrid materials," Chem. Soc. Rev. **41**, 5131–5142 (2012).
[13] P. Feng, X. Bu, and D. J. Pine, "Control of pore sizes in mesoporous silica templated by liquid crystals in block copolymer-cosurfactant-water systems," Langmuir **16**, 5304–5310 (2000).
[14] T. Kimura, S. Saeki, Y. Sugahara, and K. Kuroda, "Organic modification of FSM-type mesoporous silicas derived from kanemite by silylation," Langmuir **15**, 2794–2798 (1999).
[15] D. M. Antonelli and J. Y. Ying, "Synthesis of hexagonally packed mesoporous TiO_2 by a modified sol–gel method," Angew. Chem., Int. Ed. Engl. **34**, 2014–2017 (1995).
[16] P. C. A. Alberius, K. L. Frindell, R. C. Hayward, E. J. Kramer, G. D. Stucky, and B. F. Chmelka, "General predictive syntheses of cubic, hexagonal, and lamellar silica and titania mesostructured thin films," Chem. Mater. **14**, 3284–3294 (2002).
[17] S.-Y. Choi, M. Mamak, N. Coombs, N. Chopra, and G. A. Ozin, "Thermally stable two-dimensional hexagonal mesoporous nanocrystalline anatase, meso-nc- TiO_2: Bulk and crack-free thin film morphologies," Adv. Funct. Mater. **14**, 335–343 (2004).
[18] Y. Denkwitz, M. Makosch, J. Geserick, U. Hörmann, S. Selve, U. Kaiser, N. Hüsing, and R. J. Behm, "Influence of the crystalline phase and surface area of the TiO_2 support on the CO oxidation activity of mesoporous Au/ TiO_2 catalysts," Appl. Catal., B **91**, 470–480 (2009).
[19] P. Kubiak, T. Fröschl, N. Hüsing, U. Hörmann, U. Kaiser, R. Schiller, C. K. Weiss, K. Landfester, and M. Wohlfahrt-Mehrens, "TiO_2 anatase nanoparticle networks: Synthesis, structure, and electrochemical performance," Small **7**, 1690–1696 (2011).
[20] M. Rawolle, E. V. Braden, M. A. Niedermeier, D. Magerl, K. Sarkar, T. Fröschl, N. Hüsing, J. Perlich, and P. Müller-Buschbaum, "Low-temperature route to crystalline titania network structures in thin films," ChemPhysChem **13**, 2412–2417 (2012).
[21] P. Hartmann, D.-K. Lee, B. M. Smarsly, and J. Janek, "Mesoporous TiO_2: Comparison of classical sol-gel and nanoparticle based photoelectrodes for the water splitting reaction," ACS Nano **4**, 3147–3154 (2010).
[22] J. M. Szeifert, J. M. Feckl, D. Fattakhova-Rohlfing, Y. Liu, V. Kalousek, J. Rathousky, and T. Bein, "Ultrasmall titania nanocrystals and their direct assembly into mesoporous structures showing fast lithium insertion," J. Am. Chem. Soc. **132**, 12605–12611 (2010).
[23] E. Nilsson, Y. Sakamoto, and A. E. C. Palmqvist, "Low-temperature synthesis and HRTEM analysis of ordered mesoporous anatase with tunable crystallite size and pore shape," Chem. Mater. **23**, 2781–2785 (2011).
[24] C. J. Brinker, Y. Lu, A. Sellinger, and H. Fan, "Evaporation-induced self-assembly: Nanostructures made easy," Adv. Mater. **11**, 579–585 (1999).
[25] B. Elgh, N. Yuan, H. S. Cho, E. Nilsson, O. Terasaki, and A. E. C. Palmqvist, "Correlating photocatalytic performance with microstructure of mesoporous titania influenced by employed synthesis conditions," J. Phys. Chem. C **117**, 16492 (2013).
[26] B. Elgh and A. E. C. Palmqvist, "Controlling anatase and rutile polymorph selectivity during low-temperature synthesis of mesoporous TiO_2 films," J. Mater. Chem. A **2**, 3024 (2014).
[27] R. Su, R. Bechstein, L. Sö, R. T. Vang, M. Sillassen, B. Esbjörnsson, A. Palmqvist, and F. Besenbacher, "How the anatase-to-rutile ratio influences the photoreactivity of TiO_2," J. Phys. Chem. C **115**, 24287 (2011).
[28] M. Andersson, H. Birkedal, N. R. Franklin, T. Ostomel, S. Boettcher, A. E. C. Palmqvist, and G. D. Stucky, "Ag/AgCl-loaded ordered mesoporous anatase for photocatalysis," Chem. Mater. **17**, 1409 (2005).
[29] Y. Sakatani, D. Grosso, L. Nicole, C. Boissiere, G. J. de A. A. Soler-Illia, and C. Sanchez, "Optimised photocatalytic activity of grid-like mesoporous TiO_2 films: Effect of crystallinity, pore size distribution, and pore accessibility," J. Mater. Chem. **16**, 77 (2006).
[30] J. C. Yu, X. Wang, and X. Fu, "Pore-wall chemistry and photocatalytic activity of mesoporous titania molecular sieve films," Chem. Mater. **16**, 1523 (2004).
[31] M. A. Carreon, S. Y. Choi, M. Mamak, N. Chopra, and G. A. Ozin, "Pore architecture affects photocatalytic activity of periodic mesoporous nanocrystalline anatase thin films," J. Mater. Chem. **17**, 82 (2007).
[32] H. J. Pan, S. Y. Chae, and W. I. Lee, Mater. Sci. Forum **58**, 510–511 (2006).
[33] E. L. Crepaldi, G. J. de A. A. Soler-Illia, D. Grosso, F. Cagnol, F. Ribot, and C. Sanchez, "Controlled formation of highly organized mesoporous titania thin films: From mesostructured hybrids to mesoporous nanoanatase TiO_2," J. Am. Chem. Soc. **125**, 9770–9786 (2003).
[34] P. Müller-Buschbaum, "Grazing incidence small-angle X-ray scattering: An advanced scattering technique for the investigation of nanostructured polymer films," Anal. Bioanal. Chem. **376**, 3–10 (2003).
[35] A. Buffet, A. Rothkirch, R. Doehrmann, V. Körstgens, M. M. A. Kashem, J. Perlich, G. Herzog, M. Schwartzkopf, R. Gehrke, P. Müller-Buschbaum, and S. V. Roth, "P03, the microfocus and nanofocus X-ray scattering (MiNaXS) beamline of the PETRA III storage ring: The microfocus endstation," J. Synchrotron Radiat. **19**, 647–653 (2012).

[36] Y. Yoneda, "Anomalous surface reflection of X rays," Phys. Rev. **131**, 2010 (1963).
[37] P. Müller-Buschbaum, E. Bauer, O. Wunnicke, and M. Stamm, "The control of thin film morphology by the interplay of dewetting, phase separation and microphase separation," J. Phys.: Condens. Matter **17**, S363 (2005).
[38] P. Holmqvist, P. Alexandridis, and B. Lindman, "Modification of the microstructure in block copolymer–water–"oil" systems by varying the copolymer composition and the "oil" type:Small-angle X-ray scattering and deuterium-NMR investigation," J. Phys. Chem. B **102**, 1149–1158 (1998).
[39] J. Livage, M. Henry, and C. Sanchez, "Sol-gel chemistry of transition metal oxides," Prog. Solid State Chem. **18**, 259 (1988).
[40] R. Hosemann, W. Vogel, and D. Weick, "Novel aspects of the real paracrystal," Acta Crystallogr., Sect. A: Cryst. Phys., Diffr., Theor. Gen. Crystallogr. **37**, 85–91 (1981).
[41] R. Lazzari, "IsGISAXS: A program for grazing-incidence small-angle X-ray scattering analysis of supported islands," J. Appl. Crystallogr. **35**, 406–421 (2002).
[42] E. Nilsson, H. Furusho, O. Terasaki, and A. E. C. Palmqvist, "Synthesis of nanoparticulate anatase and rutile crystallites at low temperatures in the Pluronic F127 microemulsion system," J. Mater. Res. **26**, 288–295 (2011).
[43] B. B. Zermeno, E. Moctezuma, and R. Garcia-Alamilla, "Photocatalytic degradation of phenol and 4-chlorophenol with titania, oxygen and ozone," Sustainable Environ. Res. **21**, 299–305 (2011).
[44] A. M. Peiró, J. A. Ayllón, J. Peral, and X. Doménech, "TiO_2-photocatalyzed degradation of phenol and ortho-substituted phenolic compounds," Appl. Catal., B **30**, 359–373 (2001).
[45] T. Alapi and A. Dombi, "Comparative study of the UV and UV/VUV-induced photolysis of phenol in aqueous solution," J. Photochem. Photobiol., A **188**, 409–418 (2007).
[46] W. Xu, P. K. Jain, B. J. Beberwyck, and A. P. Alivisatos, "Probing redox photocatalysis of trapped electrons and holes on single Sb-doped titania nanorod surfaces," J. Am. Chem. Soc. **134**, 3946–3949 (2012).
[47] C. G. Silva and J. L. Faria, "Effect of key operational parameters on the photocatalytic oxidation of phenol by nanocrystalline sol–gel TiO_2 under UV irradiation," J. Mol. Catal. A: Chem. **305**, 147–154 (2009).
[48] C.-H. Chiou, C.-Y. Wu, and R.-S. Juang, "Influence of operating parameters on photocatalytic degradation of phenol in UV/TiO_2 process," Chem. Eng. J. **139**, 322–329 (2008).